Int. J. Bio-Inorg. Hybr. Nanomater., Vol. 3, No. 4 (2014), 219-229
ISSN Print: 2251-8533
ISSN Online: 2322-4142

International Journal of Bio-Inorganic Hybrid Nanomaterials

Significance of Chemical Decomposition of Chloroethyl Phenyl Sulfide (CEPS) using Zinc-Cadmium Oxide (ZnO-CdO) Nanocomposite

Meysam Sadeghi[1*], Sina Yekta[2]

[1] Instructor, Young Researchers and Elite Club, Ahvaz Branch, Islamic Azad University, Ahvaz, Iran
[2] Instructor, Department of Chemistry, Faculty of Basic Sciences, Islamic Azad University, Qaemshahr Branch, Qaemshahr, Iran

Received: 11 August 2014; Accepted: 15 October 2014

ABSTRACT

The zinc-cadmium oxide (ZnO-CdO) nanocomposites with different weight percentages of cadmium oxide (CdO) nanoparticles were successfully synthesized by the sonochemical method using zinc and cadmium nitrates as precursors to probe their nano-structured surfaces for the decomposition reactions of chloroethyl phenyl sulfide (CEPS) as a surrogate of sulfur mustard agent simulant. Scanning electron microscopy (SEM), energy dispersive X-ray spectroscopy (EDX), X-ray diffraction (XRD) and Fourier transform infrared spectroscopy (FT-IR) techniques were used to consider the characterization and determination of the composition of the synthesized nanocomposites. The reactions were carried out in methanol, chloroform and n-heptane solvents and monitored by Gas chromatography equipped with Flame ionization detector (GC-FID) and Gas chromatography coupled with a mass spectroscopy analyses. The GC analysis clearly demonstrated that maximum decomposition (100%) of CEPS took place on the surface of porous ZnO-25.99 wt% CdO nanocomposite catalyst in n-heptane solvent, after 6 h at room temperature (RT).

Keyword: Zinc-cadmium oxide (ZnO-CdO); Nanocomposite catalyst; Sono-chemical synthesis; Chloroethyl phenyl sulfide (CEPS); Decontamination.

1. INTRODUCTION

Chemical contamination is among the most important issues which can be manifested by widely used toxic chemicals such as agricultural pesticides and so on. Also there are increased risks of chemical contamination through the use of chemical warfare agents (CWAs) in military actions, in the case of accidents and also in terrorist attacks [1]. Among CWAs, sulfur mustard bis-chloroethyl sulfide or HD (commonly abbreviated as H for munition grade and D for distilled) with molecular formula of $(ClCH_2CH_2)_2S$ is a potential chemical war-

(*) Corresponding Author - e-mail: meysamsadeghi45@yahoo.com

fare agent which can be used by terrorist organization [2-5]. One of the most famous sulfur mustard agents is chloroethyl phenyl sulfide (CEPS). Since highly persistent HD is extremely toxic, research studies have been generally performed with less toxic analogues (simulants) like CEPS [6, 7]. The CEPS is considered as a HD simulant because it contains a single chlorine atom on the β carbon atom relative to HD as illustrated in Scheme 1.

Currently, many advances have been made to design methodologies and strategies to neutralize harmful chemical agents. The first decontaminants employed against CWAs, were bleaching powder and potassium permanganate [6]. Because of disadvantages associated with bleach solution, search for new decontaminants began after World War II. N-chloro compounds (chloramines-B, chloramines-T, trichlorocyanurate acid and sodium N, N-dichloroisocyanorate), DS2, oxon, etc. were also found to be promising, but lack of stability hindered their wide spread application [7-9].

Most of the above problems can be overcome using sorbent decontaminants. A sorbent decontaminant is a free flowing, solid material which adsorbs liquid agents tightly in its pores and degrades subsequently [3]. As in the recent years, interests have been inverted toward the application of nanomaterials and nanotechnology, more nanocrystalline inorganics such as metals and metal oxides with adsorptive and catalytic properties have been assayed as solid catalysts to replace the liquid detoxification of CWAs. The intriguing properties of nanomaterials are expected to be aroused owing to the increased fraction of surface atoms as their sizes decrease which occurs under conditions differing from those of the bulk atoms. High surface area and the reactive sites tailored in the form of edge and corner defects, unusual lattice planes and high surface to volume ratio, react in a stochiometric way that will lead to an arsenal of smart nano-

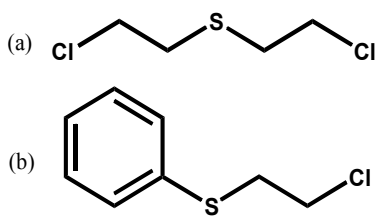

Scheme 1: *The molecular structures of: (a) HD and (b) CEPS.*

structured surfaces for specific remediation applications [10-12]. Nano-crystalline metals and metal oxides not only neutralize toxic industrial chemicals, but also destroy V-, G- and H- series CWAs through hydrolysis, hydrodehalogenation and/or hydrodesulfurization processes [13].

Several nano-crystalline metal oxides such as V_2O_5 [4], CaO [14], MgO [15-17], Al_2O_3 [15-18] and ZnO [19] have been utilized as adsorbents and catalysts for various defense applications such as nuclear, biological, chemical (NBC) warfare, destructive adsorption and decomposition of acid gases and polar organics including CWAs and their mimics [20-22]. Recently, nano-crystalline ZnO and CdO have gained increasing interests according to a variety of properties such as non-toxicity, optical and piezoelectric characteristics, and potential applications in solar energy conversion and photo-catalytic degradation of organic pollutants [23-25]. There are numerous methods for the preparation of ZnO and CdO nanoparticles including precipitation [26], hydrothermal method [27], microemulsion synthesis [28], sol-gel method [29] and sono-chemical synthesis [30]. In this research, we have proposed a simple, facile and low cost sono-chemical technique as a feasible method for the synthesis of porous ZnO-CdO nanocomposites with different weight percentages of CdO nanoparticles. Then, the nanocomposite with the optimized amount of CdO nanoparticles was investigated as the catalyst for the decomposition of CEPS.

2. EXPERIMENTAL DETAIL

2.1. Materials and reagents

Zinc nitrate hexahydrate $Zn(NO_3)_2.6H_2O$, cadmium nitrate tetrahydrate $Cd(NO_3)_2.4H_2O$, sodium hydroxide NaOH, ethanol, octane, methanol, chloroform and n-heptane all were obtained commercially from Merck, chloroethyl phenyl sulfide (CEPS) was purchased from Sigma-Aldrich. All the materials were of chemical grade and were used as received. Deionized water was used for the preparation of all solutions.

2.2. Instrumentation

Ultrasonic experiments were performed by a GM

2200 model Bandelin sonoplus (45 kHz) for the synthesis of nanocomposite samples. For the separation, samples were centrifuged via a Universal centrifuge (CAT. NO. 1004) instrument. The synthesized ZnO-CdO nanocomposites were subjected to various characterization instruments. The morphology, particle size and the element composition were determined via SEM images using a field emission scanning electron microscope fitted with an energy dispersive X-ray spectrometer (FESEM-EDX, LEO-1530VP), respectively. The X-ray diffraction (XRD) analysis was carried out on a Philips X-ray diffractometer using Cu-Kα radiation (40 kV, 30 mA and $\lambda = 0.15418$ nm). The Samples were scanned with a speed of $2°.min^{-1}$ at 2θ ranged from 10° to 90°. The IR spectra were scanned on a Perkin-Elmer model 2000 FT-IR spectrometer in the wavelength range of 450 to 4000 cm^{-1} with KBr pellets. A Varian Star 3400CX series gas chromatograph equipped with flame ionization detector (FID) and an OV-101CWHP 80/100 silica capillary column (30 m, 0.25 mm inner diameter (i.d) and 0.25 μm film thicknesses) was used to monitor the decomposition reactions of CEPS on the surface of the nanocomposite catalysts. The extracted products were analyzed by a HP-Agilent gas chromatograph-mass spectrometer equipped with a DB 1701 fused-silica capillary column (30 m, 0.25 mm inner diameter (i.d) and 0.25 μm film thicknesses). In brief, the column temperature was initially hold at 60°C for 4 min and programmed at $20°.min^{-1}$ for 13 min to 220°C to reach the final temperature which was then hold for 4 min. Helium (99.99 % purity) was selected as the carrier gas with the flow rate of 1 $mL.min^{-1}$. The detector temperature was fixed at 230°C. The injection was performed in the split mode.

2.3. Preparation of ZnO-CdO nanocomposite

ZnO-CdO nanocomposites were prepared by sonochemical method. For this purpose, initially four samples of zinc nitrate hexahydrate were prepared in 100 mL Erlenmeyer flasks through dissolving 3.85 g of $Zn(NO_3)_2.6H_2O$ powder into 10 mL of deionized water (1.29 molar). 0.285, 0.55, 1.1 and 2.2 g of $Cd(NO_3)_2.4H_2O$ powder were then added to above solutions, respectively. While the mixtures were being heated and stirred magnetically with 70°C then 100 mL of 1 M KOH aqueous solution was added drop-wise at 70°C for 60 min. Additionally, 1 M of NaOH aqueous solution was added drop-wise to precursor solutions under vigorous stirring, whereupon the samples turned into white gels. The addition of NaOH was continued until the gels vanished and white precipitates formed. The resulting precipitates were separated from solutions by centrifugation, and then sonicated for 60 min in an ultrasonic bath. After the sonication, the precipitates cooled to room temperature, then filtered and washed with deionized water and ethanol three times to remove –OH groups from their surfaces. Subsequently, the clean precipitates were dried in an oven at 60°C for 12 h and calcined in a furnace at 200°C for 1 h to obtain ZnO-CdO nanocomposite powders.

2.4. Decomposition procedure of CEPS with ZnO-CdO nanocomposite catalyst

In order to investigate the decomposition reactions, ZnO-CdO-CEPS samples were prepared according to the following procedure; 10 μL of octane as the internal standard and 10 μL of CEPS were added to 5 mL of each solvents (methanol, chloroform and n-heptane) representing the optimizing work solutions, in a 20 mL Erlenmeyer flask which was sealed to prevent the vaporization of the solvents. All samples were vortexes for 1 min to give blank samples. 0.4 of ZnO-CdO nanocomposite powder was then added to above solutions. No efforts were made to control ambient light or humidity. To achieve a perfect adsorption and a complete reaction between nanocomposite catalyst and sulfur mustard simulant through optimizing various shaking times, all samples were shaken on a wrist-action shaker for respectively 0, 1, 2, 3, 6 and 12 h. Finally 10 μL of all solution samples was extracted by a micro-syringe and injected to GC and GC-MS instruments for quantitative analysis.

3. RESULTS AND DISCUSSION

3.1. Scanning electron microscopy (SEM)

The morphology, structure and particle size of the as-synthesized catalyst samples were surveyed through magnification by SEM images for the 2.29 wt%

(Figures 1a and 1b), 5.54 wt% (Figures 1c and 1d), 16.43 wt% (Figures 1e and 1f), and 25.99 wt% (Figures 1g and 1h) of CdO, respectively. The SEM images show the approximately spherical shape and homogeneous morphology of the particles and denote that increasing CdO content does not leave any changes in the topology of the catalytic surface. Furthermore, using the described synthesis method yields ZnO-CdO composites within nano-metric scale (less than 100 nm). The presence of some bigger particles in the images is attributed to the aggregation or overlapping of some smaller particles. The average particle sizes in SEM images are consistent to a good extent and agreement with those calculated from XRD peak patterns.

3.2. Energy dispersive X-ray spectroscopy (EDX) analysis

Energy dispersive X-ray (EDX) analysis was performed to confirm the presence of zinc and cadmium

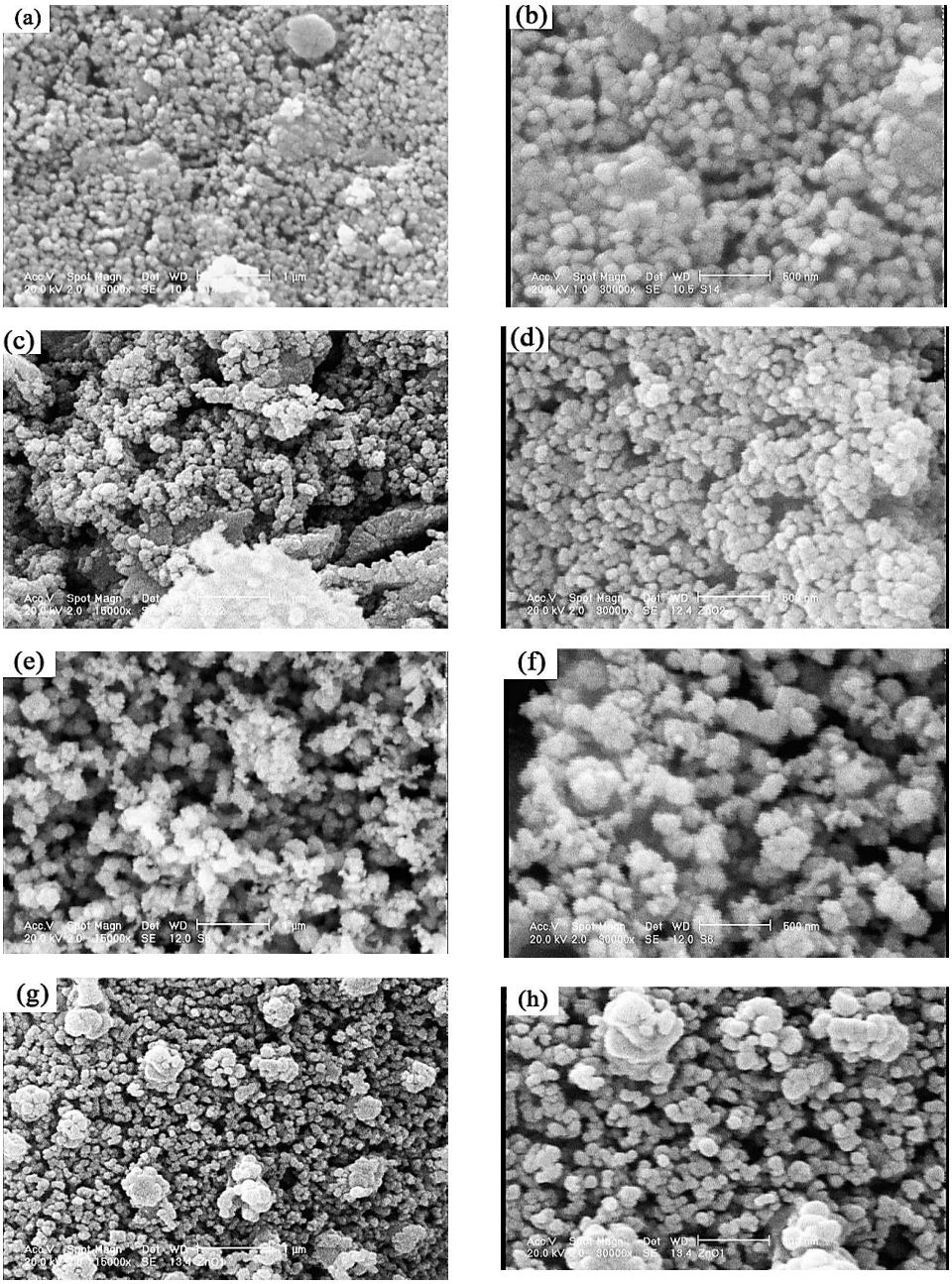

Figure 1: *SEM images of ZnO-CdO nanocomposites, (a) and (b) 2.29 wt%, (c) and (d) 5.54 wt%, (e) and (f) 16.43 wt%, (g) and (h) 25.99 wt% with different resolutions (15000X and 30000X).*

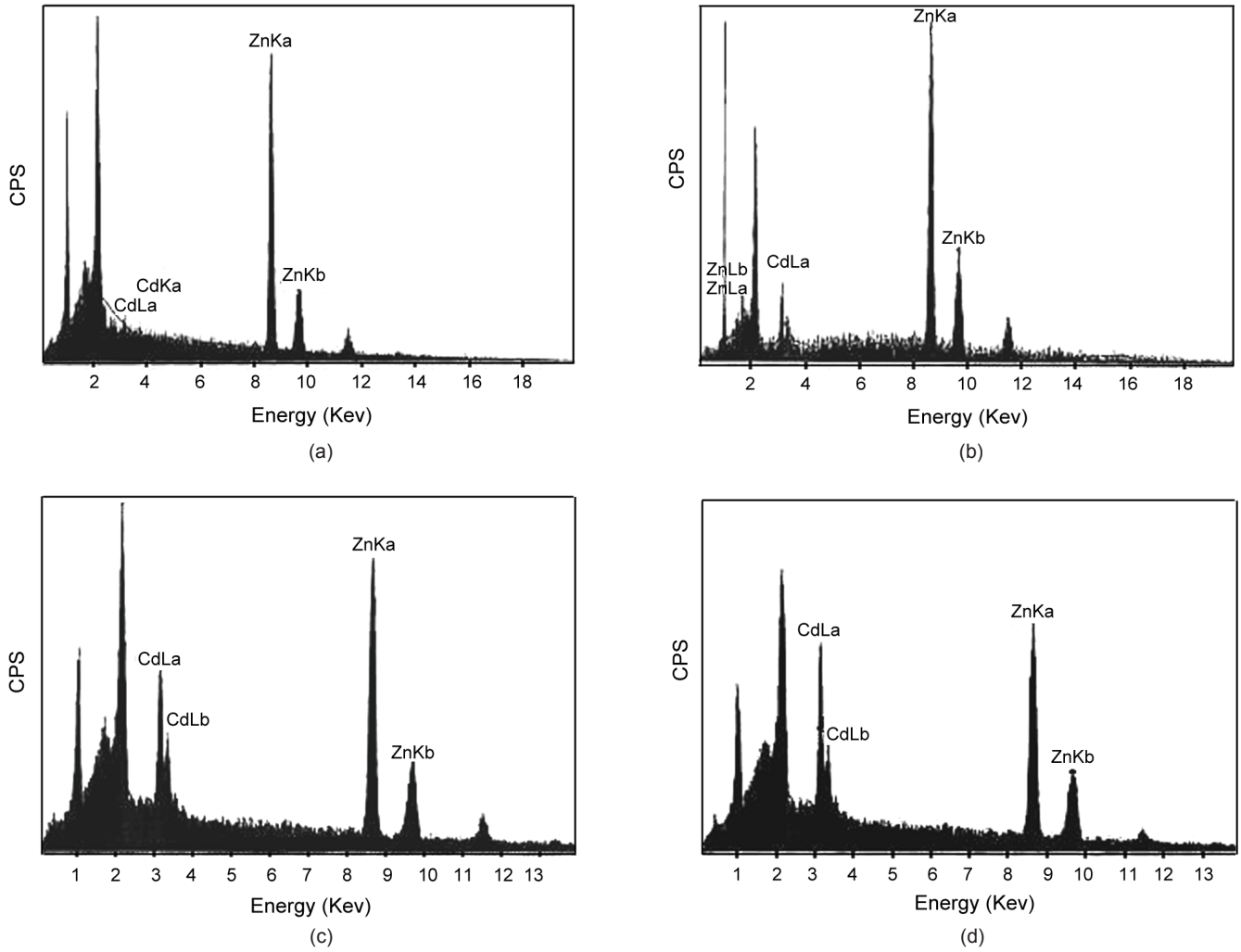

Figure 2: *EDX spectra of ZnO-CdO nanocomposites, (a) 2.29 wt%, (b) 5.54 wt%, (c) 16.43 wt%, and (d) 25.99 wt%.*

elements in nanocomposite samples and the results are shown in Figure 2. As illustrated in Figure 2, there is no unidentified peak observed in EDX spectra. These results confirm the purity and composition of ZnO-CdO nanocomposite and also obtain the amounts of CdO content as weight percent within the nanocomposite structures. These amounts are equal to 2.29 wt% (Figure 2a), 5.54 wt% (Figure 2b), 16.43 wt% (Figure 2c), and 25.99 wt% (Figure 2d), respectively.

3.3. X-ray diffraction (XRD) patterns

The structure and average particle size of the synthesized ZnO-CdO nanocomposite samples have been assayed via X-ray diffraction (XRD) measurement. As shown in Figure 3, the sharp and narrow peaks at scattering angles of 2θ of 31.72°, 34.4°, 36.24°, 47.52°, 56.6°, 62.8°, 66.3°, 67.9° and 69.1° corresponding to diffraction planes of (100), (002), (101), (102), (110), (103), (200), (112) and (201), respectively and are related to ZnO and the peaks at 2θ of 33.001°, 38.285°, 55.258°, 65.91°, 69.288° and 82.5° are corresponded to CdO with diffraction planes of (111), (200), (220), (311), (222) and (400), respectively. These peaks which are illustrated as square points in Figure 3a, 3b, 3c and 3d reveal the CdO crystals. Also the patterns have clearly indicated that the samples have not been synthesized as single phases but as a composite. The diffraction peaks appeared for all XRD patterns can be indexed with standard patterns of ZnO (a wurtzite structure and hexagonal phase with lattice constants, a = 3.24982(9) Å and c = 1.6021 Å, JCPDS card NO. 79-207) and CdO (FCC phase, JCPDS card NO. 75-293). The average particle size of nanocomposites was calculated from line broadening of the peak at 2θ =

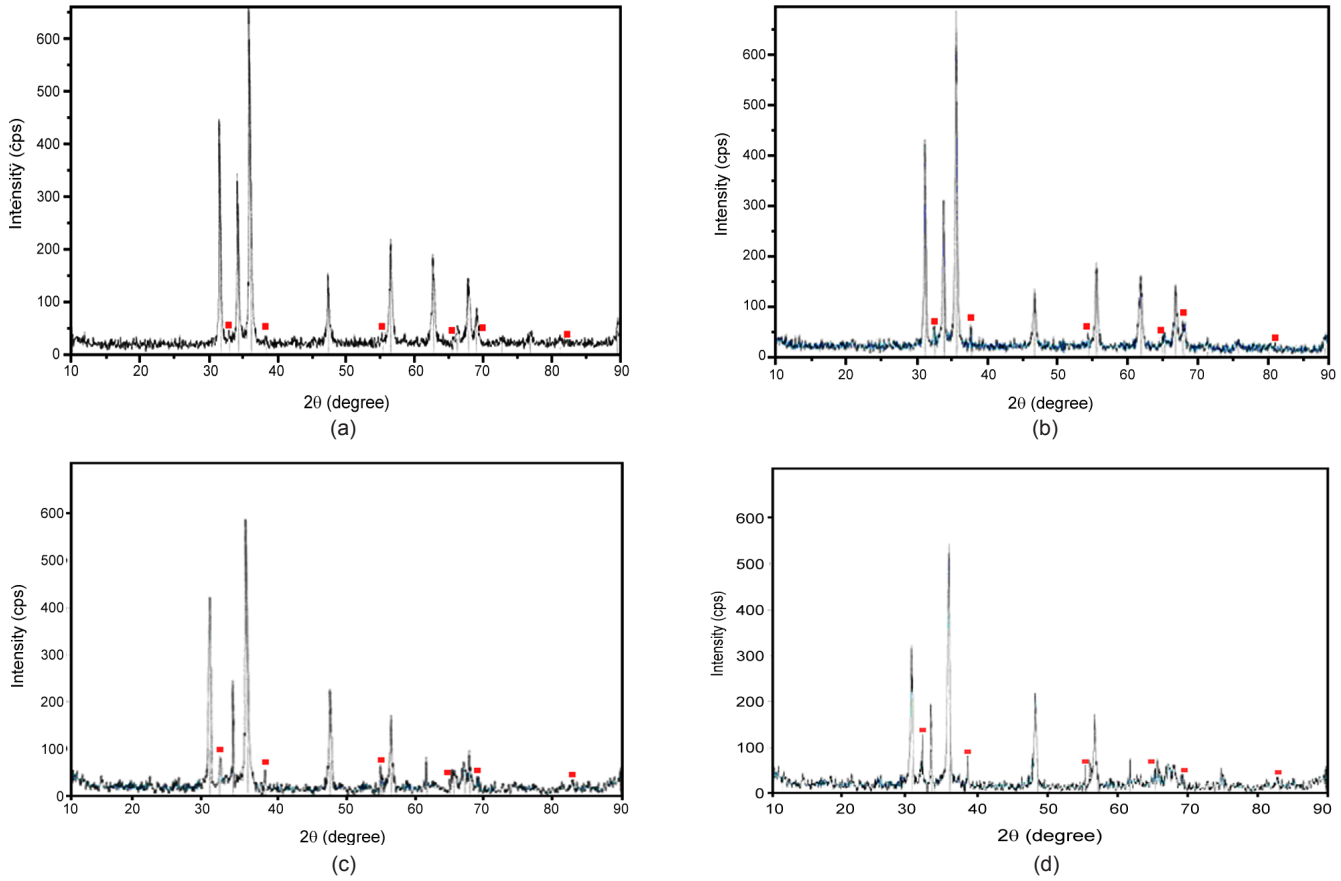

Figure 3: *XRD patterns of the synthesized ZnO-CdO nanocomposite, (a) 2.29 wt%, (b) 5.54 wt%, (c) 16.43 wt% and (d) (h) 25.99 wt% (■ indicates peak pattern depicting presence of CdO).*

10-90° using Scherrer equation (1) [31]:

$$d = \frac{0.94\lambda}{\beta \cos\theta} \quad (1)$$

Where d is the crystalline size, λ is the wavelength of X-ray source, β is the full width at half maximum (FWHM) and θ is the angle of incidence for the selected diffraction peak (Bragg diffraction angle). Using Scherrer equation, the average particle sizes of ZnO-CdO nanocomposites with 2.29 (Figure 3a), 5.54 (Figure 3b), 16.43 (Figure 3c) and 25.99 wt% (Figure 3d) CdO were estimated to be about 44.6, 49.3, 47 and 42 nm, respectively.

3.4. FT-IR study

The investigation of the presence of functional groups on the surfaces of synthesized nanocomposite catalysts was acceded by FT-IR spectra, as shown in Figure 4 in which the strong absorbed peaks around 450 cm^{-1} verify the formation of Zn–O and Cd–O bonds. The peaks at 847 and 1350 cm^{-1} are assigned to C–H and C–C bonding vibrations in the synthesized samples, respectively. There are bands in the regions 1630 and 1710 cm^{-1} which are presented probably due to the adsorbed CO_2 and moisture by samples or potassium bromide (KBr) pellets or due to traces of the remained

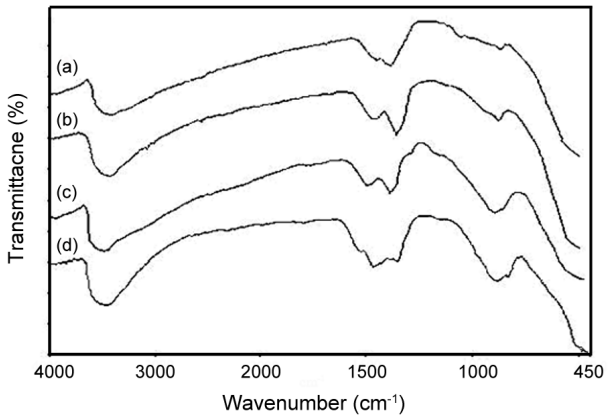

Figure 4: *FTIR spectra of ZnO-CdO nanocomposites (a) 2.29 wt%, (b) 5.54 wt%, (c) 16.43 wt% and (d) 25.99 wt% of CdO.*

solvent on the surface of metallic cations in the powders. The peaks positioned around 3460 cm^{-1} is corresponded to hydroxyl (O–H) stretching vibrations. FT-IR spectra are shown for the 2.29 wt% (Figure 4a), 5.54 wt% (Figure 4b), 16.43 wt% (Figure 4c), and 25.99 wt% (Figure 4d), respectively. After the characterization of the samples, ZnO-CdO nanocomposite with the highest amount of CdO nanoparticles (25.99 wt%) was selected due to higher amounts of cadmium oxide and smaller crystal particle size, to decontaminate the chemical warfare agent simulant of CEPS.

3.5. Catalytic study

3.5.1. GC-FID analysis

In order to study the chemical decomposition of chloroethyl phenyl sulfide (CEPS) as a surrogate of sulfur mustard agent, the catalytic performance of porous ZnO-CdO nanocomposite with 25.99 wt% CdO nanoparticles content was evaluated at room temperature and those progresses were monitored by GC-FID analysis. To accede maximum efficiency, the influencing parameters such as solvent type and shaking time have been explored and optimized. The effect of polarity on the reaction procedure and the choice of solvent type were discussed through utilizing methanol, chloroform and n-heptane.

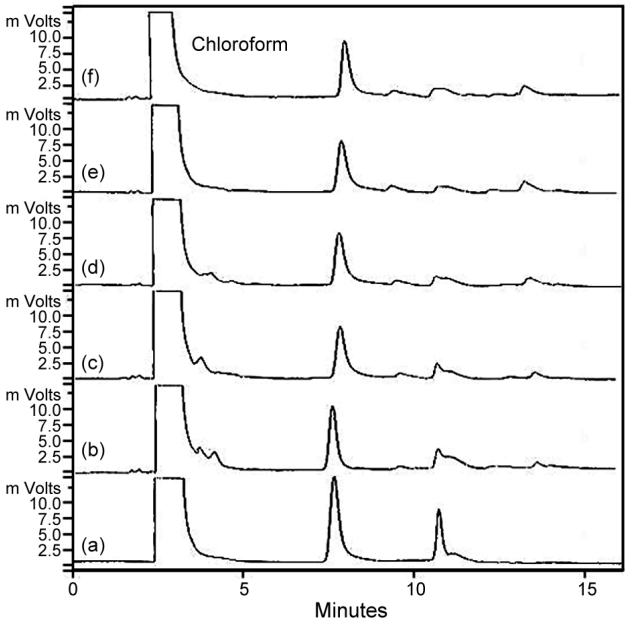

Figure 6: *GC chromatograms for ZnO-CdO-CEPS sample in chloroform solvent, a) 0 h, b) 1h, c) 2 h, d) 3 h, e) 6 h and f) 12 h.*

The GC chromatograms, area under curve (AUC) data and the results under different solvents and shaking times are summarized in Figures 5 to 8. It is observed from GC chromatograms that CEPS has a retention

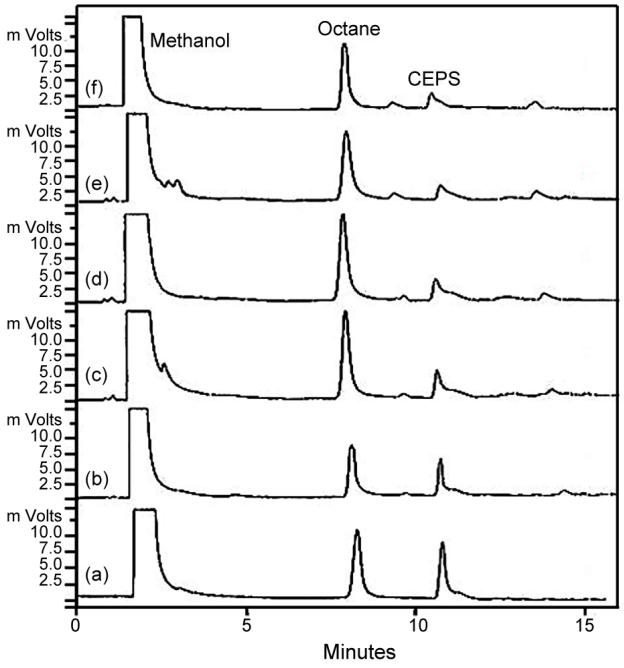

Figure 5: *GC chromatograms for ZnO-CdO-CEPS sample in methanol solvent, a) 0 h, b) 1h, c) 2 h, d) 3 h, e) 6 h and f) 12 h.*

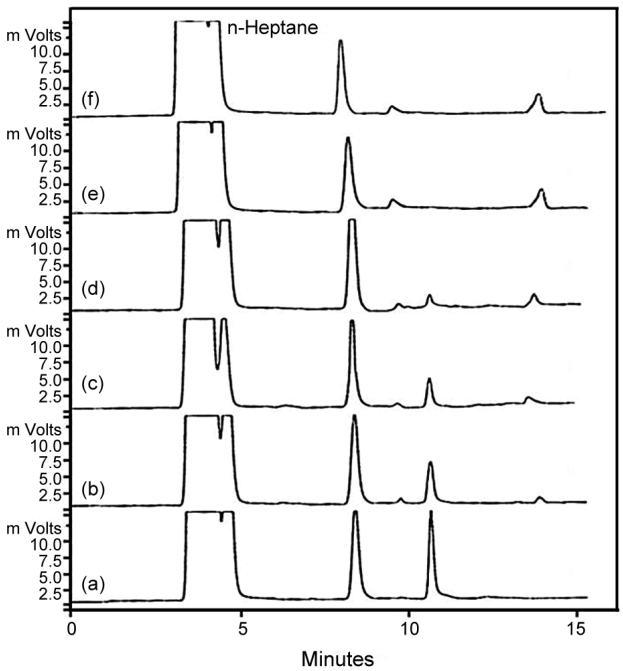

Figure 7: *GC chromatograms for ZnO-CdO-CEPS sample in n-heptane solvent, a) 0 h, b) 1h, c) 2 h, d) 3 h, e) 6 h and f) 12 h.*

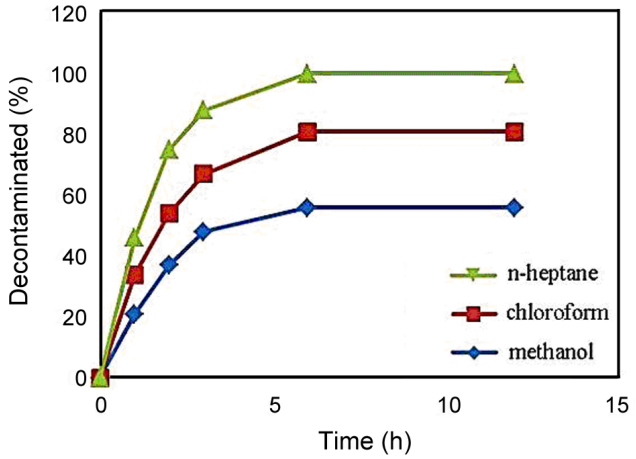

Figure 8: *The curve of decontaminated CEPS% versus reaction time in different solvents.*

time at about 10.6 min. To calculate the amounts of decomposed sulfur mustard stimulant, the integrated area under peak data of two samples, CEPS and octane as the internal standard have been given for all times and solvents. Subsequently, the ratio of the integrated data (integrated AUC of CEPS/integrated AUC of octane) was determined. The experiments were performed at different time intervals from a, b, c, d, e and f that are corresponded to 0, 1, 2, 3, 6 and 12 h from Figures 5 to 8. With increasing the time, AUC amounts of CEPS were firstly increased until 6 h, and then a constant trend was observed. It is noticed from chromatograms that with increase in the reaction (shaking) time, higher amounts of CEPS would be decontaminated which are illustrated by the new peaks at retention times of 9.7 and 14.5 min. Moreover, the experiments have clearly demonstrated that the maximum decomposition occurred in n-heptane solvent after 6 h. not with standing the transition state must be involved in the polar reaction, polar solvent hinders the reaction's progress. It could be construed from GC analysis that polar solvent can compete with the reactive sites presented on the surface of ZnO-CdO nano-

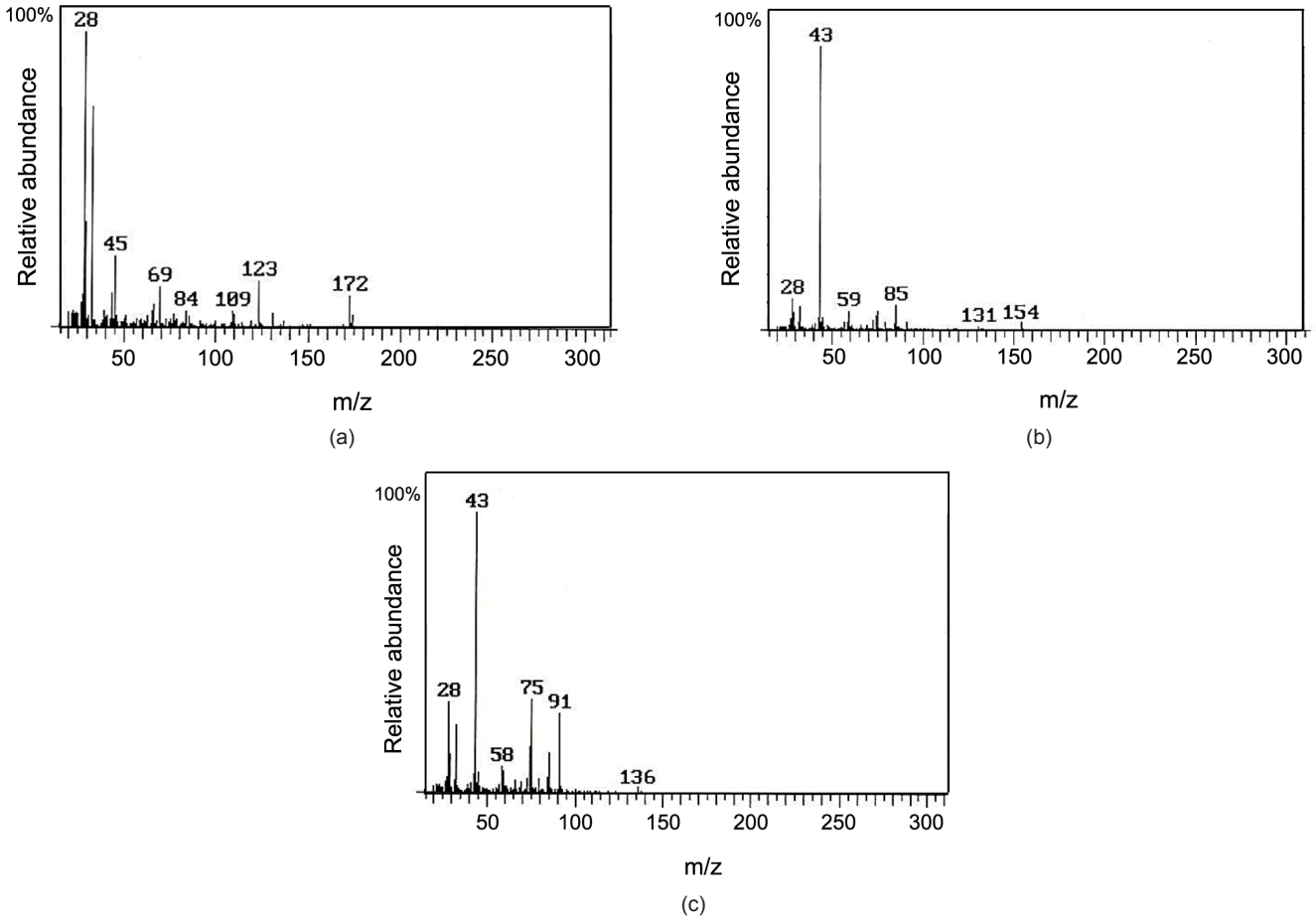

Figure 9: *GC-MS analysis and mass spectra of the reaction products ZnO-CdO nanocomposite with CEPS, a) CEPS, b) HEPS and c) PVS.*

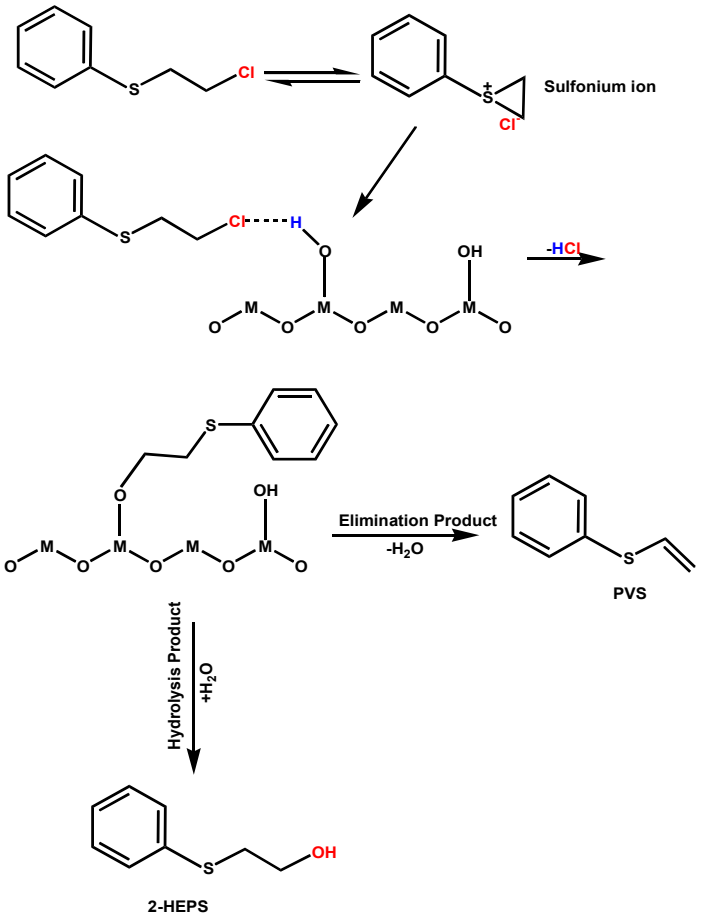

Scheme 2: *Proposed decomposition mechanism of ZnO-CdO nanocomposite exposed to CEPS (M= Zn and/or Cd).*

composite including Bronsted and Lewis acid sites. In particular, the blocking of Lewis acid sites would hinder the coordination of CEPS. Since methanol is considered as such a strong hindrance to the reaction, this tends to lend further support to the idea that methanol simply blocks access to the surface of the catalyst.

3.5.2. GC-MS analysis

Once CEPS reacted with ZnO-CdO nanocomposite catalyst, the identification and quantification of the decomposition products was followed by GC-MS analysis. Figures 9a, 9b and 9c depicts the mass spectra for CEPS (m/z values ranged from 28, 45, 69, 84, 109, 123 and 172), hydroxyl ethyl phenyl sulfide (HEPS) (m/z values ranged from 28, 43, 59, 85, 131 and 154) as hydrolysis product and phenyl vinyl sulfide (PVS) (m/z values ranged from 28, 43, 58, 75, 91 and 136) as elimination product, respectively. The formation of HEPS and PVS emphasizes the role of hydrolysis and elimination reactions in the decomposition of CEPS, thereby rendering its less-toxic products.

3.6. Mechanism of the decomposition procedure

Based on the observations provided by GC and GC-MS analyses, the mechanism schemes reflecting the decomposition (adsorption and destruction) of the sulfur mustard simulant on the adsorbent catalyst along with the formation of destruction products are proposed (Scheme 2) in which the decomposition reactions through both Zinc and cadmium species (Zn^{2+} and Cd^{2+}) have been reviewed. It is worth noting that one of the proposed routes is possible and may proceed simultaneously.

In this route, adsorption reactions of sulfur mustard simulants occur through nucleophillic attack of the Bronsted (hydroxyl groups (Zn-OH) and/or (Cd-OH)) acid sites presented on the ZnO-CdO of the external surface of the composite to chlorine and sulfur atom of CEPS molecule (initially, cyclic sulfonium ion seems

to be formed as an intermediate which is in the non-volatile form of the related compound so that could not be extracted out and detected by GC). Shortly after that, the chlorine atom in CEPS molecule will be removed through the dehalogenation reaction. In the presence and absence of H_2O molecule, different reactions may proceed and hydrolysis and elimination products on the surfaces of Zn^{2+} and Cd^{2+} as Lewis acid sites will be revealed. Both hydrolysis and elimination processes take place to yield hydroxyl ethyl phenyl sulfide (HEPS) and phenyl vinyl sulfide (PVS) as decomposition products of CEPS.

4. CONCLUSIONS

In the present study, ZnO-CdO nanocomposite with different weight percentages of CdO nanoparticles have been synthesized by sonochemical method with the goal to convert chloroethyl phenyl sulfide (CEPS) as a sulfur mustard stimulant to the chemical warfare agent, HD, to less-toxic products. Those physicochemical properties of the nanocomposite were characterized and identified by SEM, EDX, XRD and FT-IR techniques. Thereafter, ZnO-CdO nanocomposite with 25.99 wt% CdO nanoparticles was selected for studying the decomposition reactions of CEPS. Adsorption and decomposition reactions have been evaluated in different solvents and shaking times and monitored by GC and GC-MS analyses. Maximum decomposition (100%) occurred in n-heptane solvent after 6 h, compared to methanol and chloroform (56% and 81%, respectively). It is realized from experiments that polar solvent hinders the access to the active sites on the surface of nanocomposite. The results showed that ZnO-CdO nanocomposite serves as a promising catalyst for the efficient decomposition of CEPS molecule by forming less-toxic hydrolysis and elimination products.

ACKNOWLEDGMENT

The authors acknowledge department of chemistry, Imam Hussein Comprehensive University (IHCU), Tehran, Iran for his constructive advice in this research.

REFERENCES

1. Szinicz L., *Toxicology*, **214** (2005), 167.
2. Lee S.C. et al., *Sens. Actua*, **138** (2009), 446.
3. J.L. McWilliams, R.J. Steel, 1985. *Gas! The battle for Ypres*, Vanwell Publishing Limited; Deyell Co., Canada.
4. Singh B., Mahato T.H., Srivastava A.K., Prasad G.K., Ganesan K., *J. Hazard. Mater*, **190** (2011), 1053.
5. Yang Y.C., Baker J.A., Ward J.R., *Chem. Rev.*, **92** (1992), 1729.
6. Kleinhammes A. et al., *Chem. Phy. Lett.*, **411** (2005), 81.
7. Ringenbach C.R., Livingston S.R., Kumar D., Landry C.C., *Anal. Chem. Mater.*, **17** (2005), 5580.
8. Tang H., Cheng Z., Zhu H., Zuo G., Zhang M., *Appl. Catal. B: Environ*, **79** (2008), 323.
9. J.B. Jacson, 1960. CWLR, 2368, *Development of Decontamination Solution DS-2*, John Wiley and Sons: New York.
10. K.J. Klabunde, Ed., 2001. *Nanoscale Materials in Chemistry*, John Wiley and Sons: New York.
11. Klabunde K.J. et al., *J. Phys. Chem.*, **100** (1996), 12142.
12. J.A. Rodriguez, G.M. Fernandez, 2007. *Synthesis Properties and Applications of Oxide Nanomaterials*, John Wiley and Sons: New York.
13. Wagner W., Procell R., Koper B., Klabunde J., *J. Am. Chem. Soc.*, **891** (2005), 139.
14. Wagner G.W., Koper O.B., Lucas E., Decker S., Klabunde K.J., *J. Phys. Chem.*, **104** (2000), 5118.
15. Dadvar S., Tavanai H., Morshed M., Ghiaci M., *Sep. Purif. Technol.*, **114** (2013), 24.
16. Wagner G.W., Bartram P.W., Koper O., Klabunde K.J., *J. Phys. Chem.*, **103** (1999), 3225.
17. Prasad G.K. et al., *Micropor. Mesopor. Mater*, **106** (2007), 256.
18. Wagner G.W. et al., *J. Am. Chem. Soc.*, **123** (2001), 1636.
19. Mahato T.H., Prasad G.K., Singh B., Acharya J., Srivastava A.R., Vijayaraghavan R., *J. Hazard. Mater*, **165** (2009), 928.
20. Hosono H., *Thin solid films*, **515** (2007), 6000.
21. Vidyasagar C.C., ArthobaNaik Y., Venkatesh T.G.,

Viswanatha R., *Powder Technol.*, **214** (2011), 337.
22. Klingshirn C., *Chem. Phys. Chem.*, **8** (2007), 782.
23. Zou B.S., Volkov V.V., Wang Z.L., *Chem. Mater*, **11** (1999), 3037.
24. Call R.L., Jaber N.K., Seshan K., Whyte T.R., *Sol. Energ. Mater.*, **2** (1980), 373.
25. Santana G., Morales-Acevedo A., Vigil LidiceVaillant O., Cruz F., Gerardo Contreras-Puente., *Thin Films*, **373** (2000), 235.
26. Varghese N., Panchakarla L.S., Hanapi M., Govindaraj A., Rao C.N.R., *Mate. Res. Bull.*, **42** (2007), 2117.
27. Liu Y., Yong C., Xiao F., *J. Hazard. Mater.*, **163** (2009), 1310.
28. Xu C., Ni Y., Zhang Z., Ge X., Ye Q., *Mater. Lett.*, **57** (2003), 3070.
29. Dagdelen F., Gupta Z.R.K., Yakuphanoglu F., *Mater. Lett.*, **80** (2012), 127.
30. Safarifard V., Morsali A., *Ultrason. Sonochem*, **19** (2012), 1227.
31. Patterson A., *Phys. Rev.*, **56** (1939), 978.